Percolation, sliding, localization and relaxation in glassy circuits

DH and DC

Department of Physics, Ben-Gurion University of the Negev, Beer-Sheva, Israel

There is recent interest in "glassy" systems that have log-wide distribution of relaxation rates [1]. For example we note recent works regarding electron dynamics where the effective model is essentially the same as a *random walk on a disordered lattice* [2, 3]. In such type of model there is a percolation-related crossover to sub-diffusion (in one dimension), or to variable-range-hopping type diffusion (in general) [4]. This crossover is reflected in the spectral properties of the system. An similiar point of view regarding percolation is the continuous time random walk (CTRW) with a broad distribution of waiting times [5].

The more general problem of *random walk in random environment*, where transitions between sites are allowed to be asymmetric, has been explored by Sinai [6], Derrida [7], and followers [5, 8]. Focusing on one-dimensional systems, it turns out that for any small amount of disorder an unbiased spreading becomes sub-diffusive. For bias that exceeds a non-zero threshold there is a *sliding transition*, and the drift velocity becomes non-zero. This type of dynamics is relevant to studies in a biophysical context: pulling pinned polymers, DNA denaturation [9, 10], population biology [11, 12], and molecular motors [13, 14]. The bias in the case of depinning polymers and DNA denaturation is the pulling force. In the case of population biology, it is the drift velocity of the nutrients and for molecular motors it is the affinity of the chemical cycle. The sliding transition is a major theme in the latter context.

Considering a finite system, the prototype being an N-site ring, one asks what are the relaxation modes of such a topologically closed system. In the Brownian motor context N is the length of a cycle, i.e. the number of chemical reactions required to advance the motor by one step. In the remaining examples, sites have a spatial context and the number of sites N arises from discretisation.

A complementary question regarding the "delocalization" of eigenstates of non-Hermitian quantum Hamiltonians has been addressed by Hatano, Nelson, and followers [15–17], originally in the context of vortex depinning in type II superconductors. In this case, the bias is the applied transverse magnetic field and N is the number of defects to which the magnetic vortex can pin. Their main achievement is the realization that the complex spectrum of the non-Hermitian hamiltonian can be deduced from the real spectrum of an associated Hermitian hamiltonian. Various improvements on the method and ensuing analytical results were obtained. For example, the complex spectrum in the thermodynamic limit was found in [18]. An equation for the curve in the complex plane on which the eigenvalues are located and the density of states was found in [19]. Results for special models of one impurity and one way dynamics (maximally asymmetric transition rates) were obtained in [20].

We show below that for a conservative "random walk" dynamics the implied spectral properties are dramatically different. Notable "conservative random walkers" are Brownian motors. For example, molecular motors on heterogeneous tracks, such as DNA or RNA. In [13, 14] non conservative motors are considered. It was found that under an external force and strong disorder, the motor will become localized at preferred positions yet near the stall force, localization occurs for any amount of disorder. These results were obtained by observing the numerically obtained spectrum.

To summarize [14], they use a different method, bypassing the hermitization procedure. The long time behavior of v and D is deduced by numerical observations of the lower edge of the spectrum (small $|\lambda|$). In fact the hermitization procedure is claimed to obscure the complexity transition (we found it!). Somehow they do not bridge between complexity of the spectrum and the sliding transition in a purely conservative model. They make some comments regarding complexity and sliding in the following respect. They consider a model where there are two types of unit cells. Each unit cell is made of two bonds. The chain is composed of unit cells drawn from a bimodal distribution. Real eigenvalues only appear due to non conservative diagonal disorder (detachment rate). They do not find an explicit crossover to complexity and do not handle the purely conservative case.

I. STOCHASTIC SPREADING

Diffusive spreading.– Einstein has considered in his thesis the problem of Brownian motion. This can be regarded as a stochastic process in which a particle hops from site to site with some hopping rate w. The rate equation can be written in matrix notation as

$$\frac{d\boldsymbol{p}}{dt} = \boldsymbol{W}\boldsymbol{p}, \tag{1}$$

involving a matrix $\boldsymbol{W}$ whose off-diagonal elements are the transitions rates w_{nm}, and with diagonal elements $-\gamma_n$ such that each column sums to zero. For example, in the case of a one-dimensional lattice with near-neighbor hopping

$$\boldsymbol{W} = \begin{bmatrix} -\gamma_1 & w_{1,2} & 0 & \dots \\ w_{2,1} & -\gamma_2 & w_{2,3} & \dots \\ 0 & w_{3,2} & -\gamma_3 & \dots \\ \dots & \dots & \dots & \dots \end{bmatrix} \tag{2}$$

with $\gamma_n = \sum_{m(\neq n)} w_{mn}$. Einstein's theory assumes a symmetric matrix $\boldsymbol{W}$. The diffusion coefficient is $D \sim wa^2$, where w is the average hopping rate between neighboring sites, and a is the average distance between them. The associated negative eigenvalues $\{-\epsilon_k\}$ of the matrix $\boldsymbol{W}$ are characterized by the spectral density

$$\rho(\epsilon) = \text{const } \epsilon^{\mu-1} \quad \text{(for small } \epsilon) \tag{3}$$

where $\mu = d/2$, and $d = 1,2,3$ is the dimensionality. It is physically appealing to think of W as the Hamiltonian matrix of a particle on a lattice, and then $-\epsilon_k$ are the eigen-energies. Optionally the w_{nm} may represent spring-constants, and then $\omega_k = \sqrt{\epsilon_k}$ are the Debye frequencies of the vibrational modes.

Percolation transition.– The first question that arises is how is Einstein's result affected if the rates come from some wide distribution. The simplest model assumes randomly distributed sites, and rates that depend exponentially on the distance $w \propto \exp(-r/\xi)$. For such a type of model the distribution of the rates is

$$P(w) = \text{const } w^{\alpha-1} \quad \text{(for small } w) \tag{4}$$

where $\alpha = \xi/a$. If the distance between the sites is increased, α decreases. As the network becomes "glassy" ($\alpha < 1$) there is a percolation-related transition to very slow diffusion ("variable range hopping"). This holds for any dimension $d > 1$. For one dimension ($d = 1$) there is a more dramatic transition to sub-diffusion. In the later case the spectral density is no longer $\mu = d/2 = 1/2$, but ([21])

$$\mu[\text{of symmetric matrix}] = \min\left\{ \frac{\alpha}{1+\alpha} , 1/2 \right\} \tag{5}$$

Sinai spreading.– The second question that arises is what happens to Einstein's theory if the transition rates are asymmetric. This question has been addressed by Sinai, Derrida and followers, sometimes called "random walk in random environment". We define the stochastic field as

$$\mathcal{E}_{m \rightsquigarrow n} \equiv \ln\left(\frac{w_{nm}}{w_{mn}} \right), \qquad (n \neq m) \tag{6}$$

such that the ratio of "backward" to "forward" transitions equals a Boltzmann factor $e^{-\mathcal{E}}$. For the purpose of presentation we assume that the stochastic field has box distribution within $[s-\sigma, s+\sigma]$. The average value s, the so called affinity, determines the direction of the drift velocity $v = v_\sigma(s)$. It is well known that by a similarity transformation the W of an *open* chain becomes a symmetric matrix H. The associated spectrum $\{-\epsilon_k\}$ consists of real negative values, and is characterized by a spectral density $\rho(\epsilon)$ that is discussed below.

Sliding transition.– Consider a sample of N sites. For $s \ll 1/N$ the Einstein relation implies that $v/D = s$. For larger s the ratio becomes smaller, and eventually for a very large s it saturates $v/D \to 2/a_\sigma$. The length scale a_σ depends on the disorder σ, and equals the lattice constant in the absence of disorder ($a_0 = a$). In the limit $N \to \infty$ it has been established that $v_\sigma(s) = 0$ up to some critical value s_1. For $s > s_1$ the drift velocity becomes finite, which we call "sliding transition". The s dependence of the diffusion coefficient $D = D_\sigma(s)$ is more complicated: it is vanishingly small up to some value $s_{1/2}$, then it becomes infinitely large up to some critical value s_2, while for larger s it becomes finite. The sliding-transition threshold s_μ is determined solely by the μth moment of $e^{-\mathcal{E}}$, and is not affected by the $P(w)$ distribution. By inverting the relation $s = s_\mu$ we get the exponent that characterizes the spectral density $\rho(\epsilon)$, namely

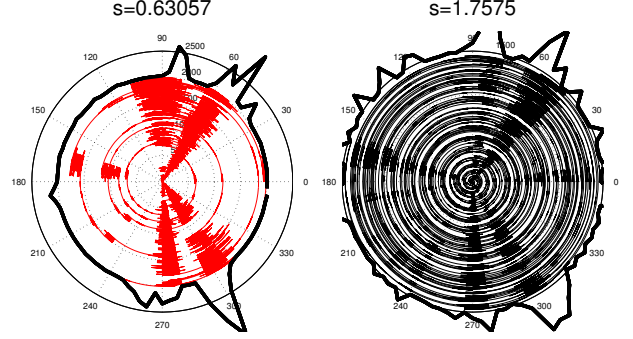$$\mu[\text{of asymmetric matrix}] = \mu_\sigma(s) \in [0,\infty] \tag{7}$$

FIG. 1. Simulated trajectory of a particle on a disordered ring. For small s (left panel) the dynamics is overdamped, while for large s (right panel) the dynamics is under damped. The radial direction is time. The thick line on the edge of the circle is the steady state distribution. For this figure there are $N = 100$ sites and $\sigma = 3$.

This implies that the spreading process is anomalous. By definition for $s > s_\infty$ we get $\mu = \infty$. For the assumed box distribution $s_\infty = \sigma$. The $\mu = \infty$ value means that a gap is opened: the lowest eigenvalue has a non-zero N-independent finite value. For zero disorder $\epsilon_0 = v^2/(4D) \propto s^2$ is the characteristic rate of drift limited relaxation, while for very large disorder $\epsilon_0 \propto \exp[(s-\sigma)/2]$ is the minimal transition rate of the network.

Relaxation.– We close an N-site chain into a ring. Now a topological aspect is added to the problem, and one wonders what are the relaxation modes of the system. It should be clear that in a closed system the lowest eigenvalue is always $\lambda_0 = 0$, while all the other eigenvalues $\{-\lambda_k\}$ have negative real part, and may have an imaginary part as well. Complex eigenvalues imply that the relaxation is not over-damped: one would be able to observe an oscillating density during relaxation, as demonstrated in Fig.1. The work of [17], regarding the dynamics that is generated by non-Hermitian quantum Hamiltonians, has considered what happens to the spectrum of a non-conservative matrix W whose diagonal elements γ_n are *fixed*. As s (as defined after equation(6)) is increased beyond a threshold value s_c, the eigenvalues in the middle of the spectrum become complex. As s is further increased beyond some higher threshold value, the entire spectrum becomes complex. In Fig.4 we see that this is not the case in our system: **(a)** The delocalization starts at the bottom of the band; **(b)** Asymptotically only a finite fraction of the spectrum becomes complex. We name the latter effect *saturation of complexity*.

II. SCOPE

Our objective is to understand how the spectral properties of the W matrix are affected as the affinity s is increased. A crucial observation is that the conservative property of the matrix implies that s affects not only the stochastic field, but also the diagonal elements. As in the work of [17] we can transform W into a non-hermitian H matrix. This matrix features the following properties: **(i)** Off-diagonal disorder character-

ized by α; **(ii)** An affinity parameter s. **(iii)** Diagonal disorder that is implied by the conservativity. It is the last property that implies a dramatically different spectral scenario. In particular we would like to address the following questions: **(1)** How does the relaxation rate of the system depend on s? **(2)** What determines the threshold s_c for getting a complex quasi-continuum? **(3)** Why is there, and what determines the saturation of complexity? **(4)** How is the sliding transition reflected in the spectrum? **(5)** How is the percolation transition reflected in the spectrum?

In order to answer the above questions we translate the spectral problem into the language of Electrostatics in the two dimensional complex plane. We first address the simplest problem of a clean N-site ring with sparse field disorder. We explain that $s_c \sim \sigma\sqrt{M}/N$, which is the field required to overcome M field defects. Then we discuss a fully disordered ring. We show how the sliding transition thresholds s_μ are expressed in the spectral properties. In particular we show that $s_c \to s_{1/2}$, which is the field required to get a sliding transition for D. For $s > s_\infty$ the real spectrum of an open chain is gapped. But for a closed ring the delocalization transition leads to a non-gapped complex λ-spectrum, that exhibits complexity saturation. We explain how the percolation-related transition affects the delocalization process.

III. OUTLINE

IV. DIFFUSION AND RELAXATION

Consider a stochastic process on an N-site ring with lattice spacing $a = 1$, that is generated by a rate equation with near-neighbor hopping as described by the matrix W of equation (2), where the site index n is defined modulo N. For convenience we use the following notations:

$$\overrightarrow{w}_n = w_{n+1,n} = w_n\, e^{+\mathscr{E}_n/2} \qquad (8)$$

$$\overleftarrow{w}_n = w_{n,n+1} = w_n\, e^{-\mathscr{E}_n/2} \qquad (9)$$

For a clean ring (no disorder) the stochastic field is uniform ($\mathscr{E} = s$) and all the couplings are the same ($w_n = w$). The drift velocity and the diffusion coefficient are

$$v_0(s) = (\overrightarrow{w} - \overleftarrow{w}) = 2w\,\sinh(s/2) \qquad (10)$$

$$D_0(s) = \frac{1}{2}(\overrightarrow{w} + \overleftarrow{w}) = w\,\cosh(s/2) \qquad (11)$$

The continuum limit is transparent, and corresponds to the solution of a diffusion equation with a drift term. It is easy to see that the eigenvalues $\{-\lambda_n\}$ of the W matrix are

$$\lambda_n = 2w\left[\cosh\left(\frac{s}{2}\right) - \cos\left(\frac{2\pi}{N}n + i\frac{s}{2}\right)\right] \qquad (12)$$

The non-equilibrium steady state (NESS) is associated with $\lambda_0 = 0$. The complexity of the other eigenvalues implies that the relaxation process in not over-damped. Even without any mathematics it is quite clear that the relaxation rate Γ is limited by the lowest diffusion mode, namely

$$\Gamma = \text{Re}[\lambda_1] = \left(\frac{2\pi}{N}\right)^2 D \qquad (13)$$

It is also physically clear that if the ring is "opened", or optionally if one of the links is removed, then the relaxation becomes drift-limited. The result is

$$\Gamma = 2w\left[\cosh\left(\frac{s}{2}\right) - 1\right] \sim \frac{v^2}{4D} \qquad (14)$$

It is important to realize that in the latter case we have a "gap" in the spectrum, meaning that λ_1 does does not diminish in the $N \to \infty$ limit.

In Fig.2 we calculate $v(s)$ and $D(s)$ for a ring with disorder, deduce from it Γ using equation (13), and compare with the numerically determined $\text{Re}[\lambda_1]$. We deduce that the non-monotonic behaviour of Γ can be explained by the known theory of the sliding transition. The question arises whether the sliding transition affects also the global properties of the spectrum. In order to address this question we have to analyze the secular equation that is associated with the matrix W.

V. THE SECULAR EQUATION

By a similarity transformation of W one obtains

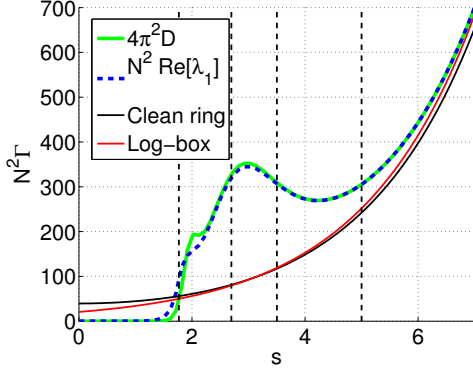$$\tilde{W} = \text{diagonal}\{-\gamma_n\} + \text{offdiagonal}\{w_n e^{\pm s/2}\} \qquad (15)$$

FIG. 2. The relaxation rate $\Gamma = \text{Re}[\lambda_1]$ versus the affinity s for $N = 1000$ sites $\sigma = 5$. The non monotonic dashed blue line has been obtained via numerical diagonalization, whereas the solid green was obtained by calculating the diffusion coefficient as in [22]. The monotonic lines correspond to the limits of clean ring (equation (13), black) and $s > s_\infty$ (equation (43), red). The vertical dashed lines are the affinities s_μ that are associated with the scaled values $\mu = 1/2, 1, 2, \infty$ (from left to right).
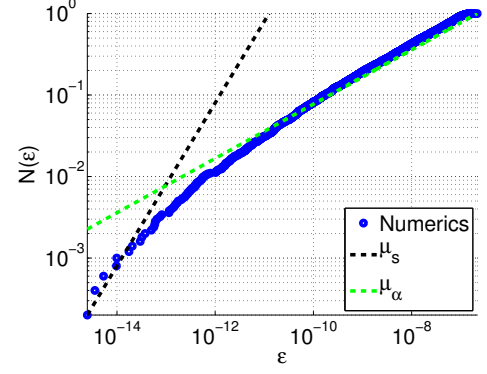

FIG. 3. The integrated density of the ϵ_k for a ring with $N = 5000$ sites. The system is characterized by a percolation exponent $\mu_\alpha = 1/3$ and a scaled affinity $\mu_s = 1$. The width of the stochastic-field distribution is $\sigma = 2$. The blue points are are results of numerical diagonalization. There is a crossover from density that corresponds to μ_s (dashed black line) to density that corresponds to μ_α (dashed green line).

where the "±" are for the "forward" and "backward" transitions respectively. Note that the statistics of the $\mathscr{E}_n$ is still hiding in the diagonal elements. The associated symmetric matrix H is defined by setting $s = 0$. Then one can define a spectral determinant $S(z)$ and associated spectrum as follows:

$$\det(z - H) = \prod_k (z + \epsilon_k) = S(z) \qquad (16)$$

If the system is an N-periodic infinite lattice, then W is similar to H by "gauge" transformation, hence one can regard the $\{-\epsilon_k\}$ as the spectrum of an open chain. But if the system is an N-periodic ring (periodic boundary conditions) then s cannot be "gauged" away. Still there is a simple relation [23] that relates the spectral determinant of W to that of H. Namely,

$$\det(z - W) = \prod_k (z + \lambda_k) \equiv S(z) - S_0 \qquad (17)$$

where

$$S_0 = 2\left[\cosh\left(\frac{Ns}{2}\right) - 1\right]\prod_n w_n \qquad (18)$$

The roots $z = -\lambda_k$ have real negative part, but may be complex in general. The lowest eigenvalue $\lambda_0 = 0$ corresponds to the non-decaying non-equilibrium steady state (NESS). It is implied that

$$S(0) = S_0 \qquad \text{implication of conservativity} \qquad (19)$$

We emphasize that the latter property is not true for a general non-Hermitian matrix, neither is the "positivity" of the λ_k. This has far reaching implications: in particular it should be clear that the NESS is an extended state, hence it follows that the localization length has to diverge in the limit $\lambda \to 0$. This is in essence the difference between the conventional Anderson model (Lifshitz tails at the band floor) and the Debye model (phonons at the band floor).

From the above it follows that the secular equation for the λ spectrum can be written as

$$\prod_k \left(\frac{z + \epsilon_k(s)}{\overline{w}}\right) = 2\left[\cosh\left(\frac{Ns}{2}\right) - 1\right] \qquad (20)$$

where $\overline{w}$ is the geometric average of all the rates. The affinity s affects both the ϵ_k and the right hand side.

VI. THE REAL SPECTRUM

The main observation regarding the real spectrum ϵ_k of the associated symmetric matrix H is that for $s < s_\infty$ it is gapless and for $s > s_\infty$ a gap opens up. This can be seen both in the spectral density and in the electrostatic potential along the real axis. Recall that $\rho(\epsilon) \sim \epsilon^{\mu-1}$. Consider first the case $\alpha \gg 1$, the percolation aspect is absent and $\mu = \mu_s$. The simplest case is for $s > s_\infty$, where a gap opens up at $\epsilon_0 = e^{(s-\sigma)/2}$ and the spectral density is distributed log-box, $\rho(\epsilon) = N/\sigma\epsilon$. This holds as long as $\alpha \gg 1$. The interesting case is when $\alpha \lesssim 1$ and $s < s_\infty$, now there is a crossover in the spectrum between two anomalous behaviours. The bottom of the band is determined by μ_s and the top of the band by μ_α, as show in Fig.3. As α decreases, the μ_s determined region becomes smaller. This crossover is analogous to regular diffusion, where there is a crossover from short time, diffusion limited spreading to long time drift limited spreading. In our case the crossover is from low energy (long time) sliding (μ_s) to high energy (short time) percolation limited diffusion μ_α.

VII. ELECTROSTATICS

In order to get an insight into the secular equation we define an "electrostatic" potential as follows:

$$\Psi(z) = \sum_k \ln\left(\frac{z - \epsilon_k}{\overline{w}}\right) \equiv V(x,y) + iA(x,y) \quad (21)$$

where $z = x + iy$. Note that compared with equation (15) we have flipped the sign convention ($z \mapsto -z$). The potential for a given charge distribution $\rho(x)$ is

$$V(x,y) = \frac{1}{2}\int \ln\left[(x - x')^2 + y^2\right]\rho(x')dx' \quad (22)$$

and along the real axis it is

$$V(\epsilon) = \int \ln(|\epsilon - x|)\rho(x)dx \quad (23)$$

The constant $V(x,y)$ curves correspond to potential contours, along which $|S(z)|$ is constant, and the constant $A(x,y)$ curves corresponds to stream lines, along which the phase of $S(z)$ is constant. The derivative $\Psi'(z)$ corresponds to the field, which can be regarded as either electric or magnetic field up to a 90deg rotation. Using this language the secular equation takes the form

$$V(x,y) = V(0); \quad A(x,y) = 2\pi * \text{integer} \quad (24)$$

Namely the roots are the intersection of the field lines with the potential contour that goes through the origin. From the preceding section we know that the potential at the origin is

$$V(0) = \ln\left[2\cosh\left(\frac{Ns}{2}\right) - 2\right] \quad (25)$$

From a straightforward electrostatic calculation we find that for a charge density that is given by equation (3) with some cutoff ϵ_c, the derivative of the electrostatic potential at the origin is given by (see supplementary material for derivation)

$$V'(\epsilon) \approx \frac{\epsilon^{\mu-1}}{\epsilon_c^{\mu}}\pi\mu\cot(\pi\mu) \quad (26)$$

Indicating that the sign changes from positive to negative at $\mu = 1/2$.

Let us make a few observations regarding the potential $V(\epsilon)$ along the real axis. For an illustration see Fig.4. Clearly if the envelope of $V(\epsilon)$ is above the $V = V(0)$ line, then the spectrum is real, and the λ_k are roughly the same as the ϵ_k, shifted a bit to the left. The second observation is that the envelope of $V(\epsilon)$ is positive in segments where the ϵ_k forms a quasi-continuum. This follows from the observation that $(1/N)V(\epsilon)$ equals the inverse localization length [17]. In the case under study the quasi-continuum starts at $\epsilon_s = 0$ for $s < s_\infty$ (Fig.4), and at finite ϵ_s for $s > s_\infty$ (Fig.6). If follows that the threshold s_c for getting a complex quasi-continuum is either $V'(0) < 0$ or $V(\epsilon_s) < V(0)$ respectively. In the former case it follows from equation (26) that $s_c = s_{1/2}$.
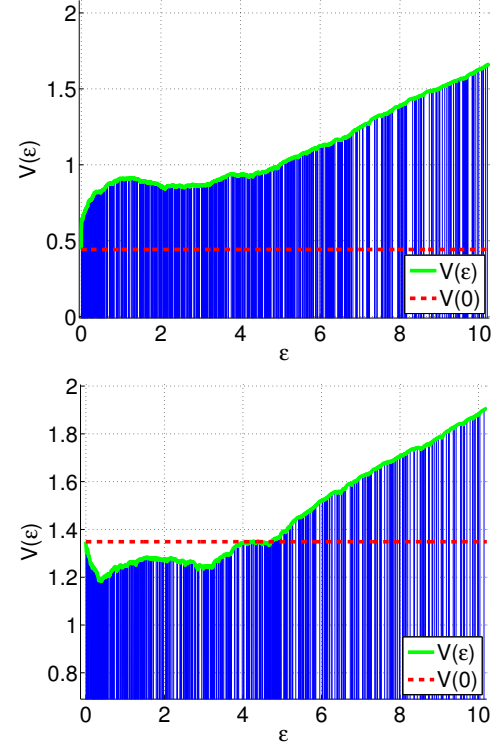

FIG. 4. The electrostatic potential $V(\epsilon)$ along the real axis. Here $N = 1000$, $\sigma = 5$. On the top panel $s < s_{1/2}$ and the spectrum is real. On the bottom panel $s > s_{1/2}$ and the spectrum becomes complex complex. For $s > s_\infty$ the real spectrum has a gap as illustrated in Fig.6a.

VIII. DETERMINATION OF s_c - WHITE VS SPARSE DISORDER

The simplest case to exhibit a crossover to a complex spectrum is that of a single defect. There are two types of defects, either in the couplings w_n or in the fields $\mathscr{E}_n$. The details are slightly different, but the analysis is essentially the same. The spectrum ϵ_k of the symmetric matrix H has two components: A continuum in the range $2\cosh(s/2) \pm 2$ and two additional states. There are two additional states because by changing a single bond, two decay rates are altered. In the language of electrostatics we have a continuous charge distribution and two point charges γ_1, γ_2. In general, one of these charges is immersed in the continuum and one of the charges is isolated, either well above or well below the continuum. Since the continuum does not contribute to the potential $V(\epsilon_s)$ (see appendix), in the end

$$V(\epsilon_s) = V_{\text{charges}} \quad (27)$$

a single charge generates the potential $V(|\gamma_i - \epsilon_s|) \approx \ln\gamma_i$ where γ_i is the position of the isolated charge. All one has to do now is find the γ_i's for the configuration he's interested in.
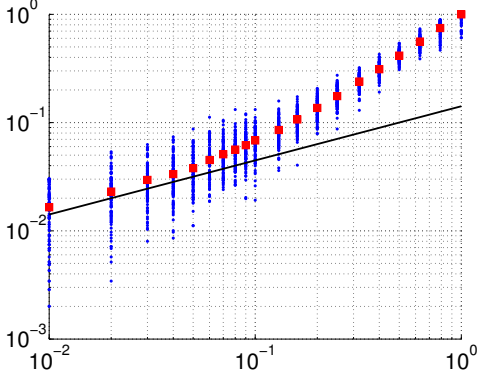
FIG. 5. The threshold value s_c for the spectrum to be complex vs. the number of stochastic field defects M. Here $N = 100$ sites and $\sigma = 5$. The x axis is the fraction of the lattice that has a disordered field, the rest of the lattice has a uniform field. For a fully disordered lattice we expect $s_c = s_{1/2}$, hence the scaling of the y axis. The black line is the sparse disorder approximation, equation (33). Blue dots correspond to 100 different realizations of disorder per M/N, red dots are their averages.

For a single defect in the stochastic field the decay rates are

$$\gamma_0 = 2\cosh(s/2) \tag{28}$$
$$\gamma_1 = e^{(s+\sigma)/2} + e^{-s/2} \tag{29}$$
$$\gamma_2 = e^{-(s+\sigma)/2} + e^{s/2} \tag{30}$$

where γ_1 is above the continuum and γ_2 is immersed in the continuum, thus $V(\epsilon_s) = \ln\gamma_1 \approx \sigma/2$, so from the condition that $V(\epsilon_s) = V(0)$ we get

$$s_c = \sigma/N \tag{31}$$

Note that this result can be obtained in the continuum limit (see Appendix).

This argument can be extended to the case of M defects, under the assumptions that the field strength of each defect is different and that the defects are well separated. If there are M field defects of varying strength $\sigma_i \in [-\sigma, \sigma]$ then there are M isolated charges $\gamma_i \approx e^{\sigma_i/2}$, so the potential is

$$V(\epsilon_s) = \sum_{i=1}^{M} \ln\gamma_i = \frac{1}{2}\sum_{i=1}^{M} \sigma_i \sim \frac{\sigma\sqrt{M}}{2} \tag{32}$$

From the condition $V(\epsilon_s) = V(0)$, one gets the threshold value

$$s_c = \frac{\sigma}{N}\sqrt{M} \tag{33}$$

Of course this approximation breaks down at some finite value of defect density M/N since the assumption that the defects are well separated is no longer valid. At this point there should be a crossover to the fully disordered behaviour where $s_c \to s_{1/2}$. In the numerics this happened at $M/N \sim 0.1$. This sparse disorder approximation is tested in Fig.5.

IX. DETERMINATION OF s_c FOR WEAK LINK

Consider now a single defect in the couplings, such that $w_1 = g$, $w_{n\neq 1} = 1$ where $g \ll 1$. In the continuum limit one

can derive the secular equation for the complex eigenvalues (see appendix)

$$\cos(k) + \frac{1}{g}\frac{k^2 + (\frac{S}{2})^2}{2k}\sin(k) = \cosh\left(\frac{S}{2}\right) \tag{34}$$

where g is the strength of the weak link and $k^2 = zL^2/D - S^2/4$ is generally complex. The envelope of the secular equation is

$$A(\lambda) = \sqrt{1 + \frac{1}{g^2}\frac{z^2}{4z - S^2}} \tag{35}$$

and is related to the electrostatic potential by $\Psi(z) = 2A(z) - 2$. This function has a minimum at $z = S^2/2$, thus the secular equation has real solutions provided

$$\sqrt{1 + \left(\frac{S}{2g}\right)^2} > \cosh\left(\frac{S}{2}\right) \tag{36}$$

The spectrum of the associated Hermitian matrix $\boldsymbol{H}$ is composed of a single state ϵ_1 and a quasi-continuum which begins at $\epsilon_s > \epsilon_1$. The single state is pushed down from the quasi-continuum such that (From numerical experiments, I still don't have the exact physical argument.) $\epsilon_s = \epsilon_1/g = s^2/4g$. The potential at ϵ_s due to the continuum is zero and the potential there, generated by ϵ_1 is (Assuming $s \ll 1$, $N \gg 1$)

$$V(\epsilon_s) = \ln\left|\frac{\epsilon_s - \epsilon_1}{g}\right| \approx \ln\left(\frac{s^2}{4g^2}\right) \tag{37}$$

Complex eigenvalues appear when $V(\epsilon_s) < V(0)$, leading to the equation for s_c

$$1 + \frac{1}{2}\left(\frac{s}{2g}\right)^2 = \cosh\left(\frac{Ns}{2}\right) \tag{38}$$

The exact equation, derived from the continuum limit (see supplementary material) is

$$\sqrt{1 + \left(\frac{s}{2g}\right)^2} = \cosh\left(\frac{Ns}{2}\right) \tag{39}$$

If there are M defects ("sparse" disorder) then there are M states that are separated from the continuum and they are equal in the vicinity of s_c (numerically verified), all to together the contribute M times to the potential $V(\epsilon_s) \approx M\ln(s^2/4g^2)$. By reverse engineering we deduce that the correct equation for s_c is

$$\sqrt{1 + \left(\frac{s}{2g}\right)^{2M}} = \cosh\left(\frac{Ns}{2}\right) \tag{40}$$

In the appendix we show that in the continuum limit the ground state is

$$\epsilon_1 = \frac{S^2}{4}\frac{g}{1-g} \tag{41}$$

so the potential at ϵ_s is

$$V(\epsilon_s) = \ln\left|\frac{\epsilon_s - \epsilon_1}{g}\right| = \ln\left[\frac{s^2}{4}\frac{1-2g}{g(1-g)}\right] \tag{42}$$

It seems that in "mixing" the electrostatic picture with the continuous problem I missed something.

X. COMPLEXITY DIMINISHES THE REAL GAP FOR $s > s_\infty$

We show that even though the real spectrum of H is gapped for $s > s_\infty$ with a quasi continuum beginning at the N-independent value $\epsilon_0 \propto \exp[(s-\sigma)/2]$, the real part of the complex gap vanishes with the system size squared but grows exponentially with s and is given by the expression

$$\Gamma \approx \frac{2\pi^2}{N^2} e^{s/2 - s_{1/2}} \cosh\left(\frac{\sigma}{2}\right) \qquad (43)$$

This estimate is tested in Fig.2. To obtain this expression we use the 2D electrostatics picture previously described. The density of states is $\rho(\epsilon) = N/\sigma\epsilon$, where $\epsilon \in [a,b]$ and $a = \epsilon_0$, $b = \exp[\sigma]\epsilon_0$. The electrostatic potential along the real axis equation (23), can be calculated analytically and is given by (see top panel of Fig.6)

$$V(\epsilon) = \ln(|\epsilon - b|)\ln\left(\frac{b}{\epsilon}\right) + \ln(|\epsilon - a|)\ln\left(\frac{\epsilon}{a}\right) + \quad (44)$$

$$+ \text{Li}_2\left(1 - \frac{b}{\epsilon}\right) + \text{Li}_2\left(1 - \frac{a}{\epsilon}\right) \qquad (45)$$

However, to determine the real part of the complex gap it is enough to realise that the equipotential contour in the complex plane, $V(x,y) = V(0)$, is approximately a parabola near the origin (see Fig.6 for an illustration). Thus, expanding equation (21) to second order near the origin, we have

$$V(x,y) \approx C_0 - C_1 x + \frac{1}{2}C_2 y^2 \qquad (46)$$

where the coefficients C_n are defined

$$C_n = \int_a^b \frac{1}{x^n} \rho(x)dx \qquad (47)$$

Notice that $C_0 = V(0)$, $C_1 = E_x(x,0)$. Since we are interested in the contour $V(x,y) = V(0)$, we obtain

$$x = \frac{1}{2}\frac{C_2}{C_1} y^2 \qquad (48)$$

For the given density of states we obtain

$$C \equiv \frac{1}{2}\frac{C_2}{C_1} = \frac{1}{2}e^{-s/2}\cosh\left(\frac{\sigma}{2}\right) \qquad (49)$$

The gap is determined by integrating the electric field, $\vec{E}(x,y) = -\vec{\nabla}V$, along the parabola of equation (48)

$$\int_0^{\sqrt{\Gamma/C}} \left|\vec{E}(x,y)\right| dy = 2\pi \qquad (50)$$

This is equivalent, through Cauchy Riemann, to the requirement $A(\Gamma,0) = 2\pi$. The integrand is approximated by $|\vec{E}(x,y)| \approx |\vec{E}(0,0)|$ by which we obtain an estimate for the gap

$$\Gamma \approx \frac{4\pi^2 C}{\left|\vec{E}(0,0)\right|^2} = \frac{2\pi^2}{N^2}e^{s/2 - s_{1/2}}\cosh\left(\frac{\sigma}{2}\right) \qquad (51)$$

XI. COMPLEXITY SATURATION FOR $s \gg s_\infty$

The secular equation for the eigenvalues is given by equation (20). In the nonconservative case, the eigenvalues of H do not depend on s, thus raising s will eventually make the entire spectrum complex. For a conservative matrix, however, $V(\epsilon)$ is also a function of s, so increasing s raises $V(\epsilon)$ at the same rate. Due to the conservative property, the eigenvalues of the associated hermitian martix, ϵ_j grow proportionaly to e^s. Increasing $s \to s + \Delta s$, we have

$$\sum_k \ln\left(\frac{z - \epsilon_k e^{\Delta s}}{w}\right) = \ln\left[2\cosh\left(\frac{(s+\Delta s)N}{2}\right) - 2\right] \quad (52)$$

$$\sum_k \ln\left(\frac{ze^{-\Delta s} - \epsilon_k}{w}\right) + N\Delta s = \ln\left[2\cosh\left(\frac{sN}{2}\right) - 2\right] + N\Delta s \quad (53)$$

but z is just a dummy variable, so we can redefine $z := ze^{-\Delta s}$ and the equation is unchanged. Thus increasing s does not change the number of complex solutions, as shown in Fig.7.

To estimate the the saturation value of the fraction of complex eigenvalues, we assume $s \gg s_\infty$. The eigenvalues have a log-box distribution so the potential along the real axis is

$$V(\epsilon) = \int_a^b \ln|\epsilon - \epsilon'|\rho(\epsilon')d\epsilon' = \qquad (54)$$

$$= \frac{N}{2\sigma}\int_{-\sigma}^{\sigma} \ln\left|e^{(s+\mathscr{E}_c)/2} - e^{(s+\mathscr{E})/2}\right|d\mathscr{E} \qquad (55)$$

Define $\mathscr{E}_c$ such that the eigenvalues with $\mathscr{E}$ in the range $-\sigma < \mathscr{E} < \mathscr{E}_c$ are complex, $\mathscr{E}_c$ is determined by the equation $V(\epsilon = e^{(s+\mathscr{E}_c)/2}) = V(0) = sN/2$, leading to

$$\int_{-\sigma}^{\sigma} \ln\left|e^{\mathscr{E}/2} - e^{\mathscr{E}_c/2}\right|d\mathscr{E} = 0 \qquad (56)$$

Clearly, $\mathscr{E}_c$ depends only on σ (and not on N) (Fig.7). The fraction of complex eigenvalues is just

$$n = \frac{\int_a^{\epsilon_c} \frac{1}{\epsilon}d\epsilon}{\int_a^b \frac{1}{\epsilon}d\epsilon} = \frac{1}{\sigma}\ln\left(\frac{\epsilon_c}{a}\right) = \frac{\mathscr{E}_c + \sigma}{2\sigma} \qquad (57)$$

The percolation transition is reflected in the complexity saturation. If $\alpha \lesssim 1$ there is saturation, but the crossover is not as sharp and the saturation value has a wider ensemble distribution, yet the upper bound is still given by equation (57). The argument for complexity saturation stems from the fact that for $s \gg s_\infty$ the matrix H is diagonal and the eigenvalues are thus log-box distributed. However when $\alpha < \infty$ the couplings are no longer equal and can be very small, thus H is no longer trivially diagonal and the eigenvalues have some complicated distribution.

In the case of a continuous system with wihite noise, the electrostatic potential is quite different [8]. It has a peculiar trait that $V(\epsilon \to \infty) = const$, the potential reaches a constant value, implying that the entire spectrum goes from real to complex at $s = s_{1/2}$, as in the bottom panel of Fig.7.
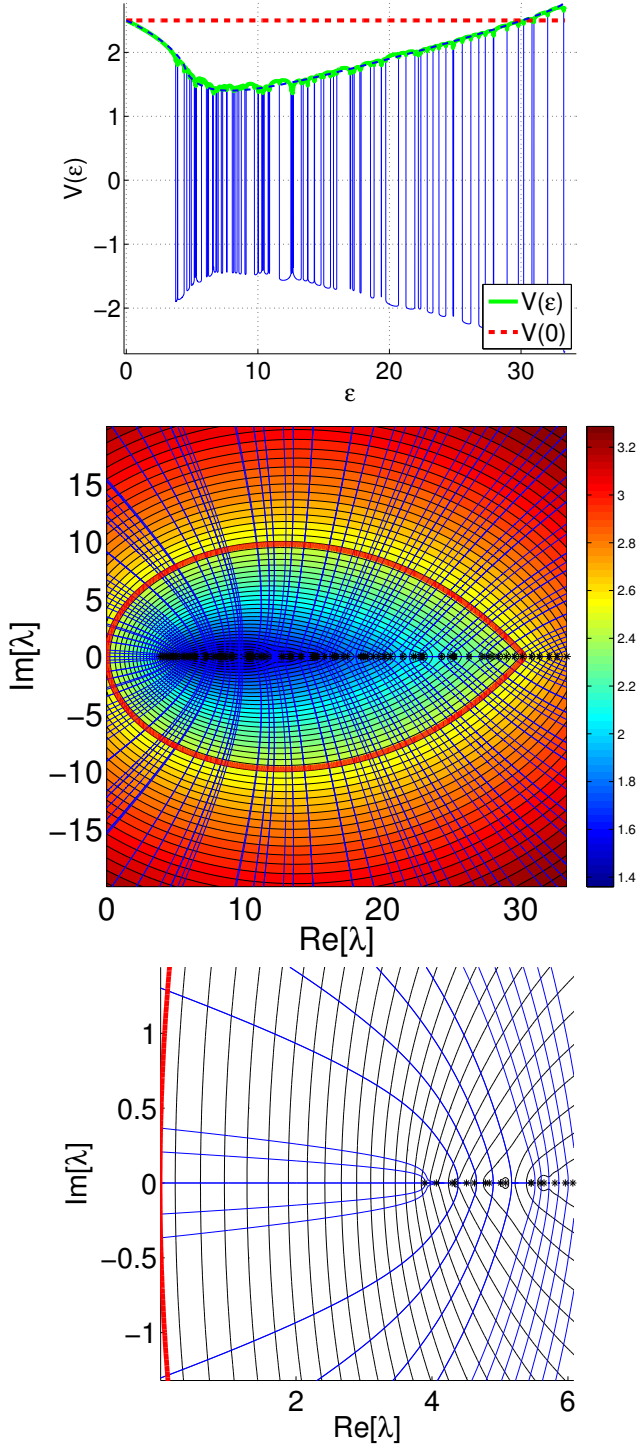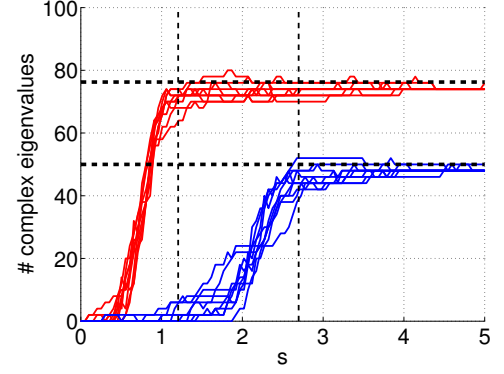
FIG. 7. We count the number of complex eigenvalues for a ring with $N = 100$ sites, for various values of the affinity s. Each red line corresponds to a different realization of field disorder with $\sigma = 3$ (red) and $\sigma = 5$ (blue). The black vertical lines are at values of $s_1(?)$ at which the sliding transition occurs. We see that the asymptotic fraction of complex eigenvalues saturates, which is quite different from what is known for non-conservative non-Hermitian matrices. The horizontal dashed line are analytical estimates of equation (57). If the lattice were continuous and the disorder white noise, the number of complex eigenvalues would go from 0 to 100 at $s = s_{1/2}$

FIG. 6. **Top panel**: The electrostatic potential $V(\epsilon)$ along the real axis. The dashed blue line is the analytical result assuming $\rho = N(\sigma x)^{-1}$, equation (44). The stars indicate the position of the "charges", which are the eigenvalues of the associated Hermitian matrix, ε_j. **Middle panel**: The electrostatic potential $\Psi(z)$ of equation (21). Here we consider a ring with $N = 100$ sites, $\sigma = 2$ and $s = 5$. The complex λ_k spectrum is obtained by looking for the intersections of the field lineswith the red thick equipotential line $V(z) = V(0,0)$ that goes through the origin. **Bottom panel**: Zoom. Note that the complex spectrum unlike the real spectrum does not have a gap.

[1] A. Amir, Y. Oreg, and Y. Imry, "On relaxations and aging of various glasses," *Proceedings of the National Academy of Sciences*, vol. 109, no. 6, pp. 1850–1855, 2012.

[2] A. Vaknin, Z. Ovadyahu, and M. Pollak, "Aging effects in an anderson insulator," *Phys. Rev. Lett.*, vol. 84, pp. 3402–3405, Apr 2000.

[3] A. Amir, Y. Oreg, and Y. Imry, "Slow relaxations and aging in the electron glass," *Phys. Rev. Lett.*, vol. 103, p. 126403, Sep 2009.

[4] Y. de Leeuw and D. Cohen, "Diffusion in sparse networks: Linear to semilinear crossover," *Phys. Rev. E*, vol. 86, p. 051120, Nov 2012.

[5] J.-P. Bouchaud and A. Georges, "Anomalous diffusion in disordered media: Statistical mechanisms, models and physical applications," *Physics Reports*, vol. 195, no. 45, pp. 127 – 293, 1990.

[6] Y. G. Sinai, "Limit behaviour of one-dimensional random walks in random environments," *Teoriya Veroyatnostei i ee Primeneniya*, vol. 27, no. 2, pp. 247–258, 1982.

[7] B. Derrida, "Velocity and diffusion constant of a periodic one-dimensional hopping model," *Journal of Statistical Physics*, vol. 31, no. 3, pp. 433–450, 1983.

[8] J. Bouchaud, A. Comtet, A. Georges, and P. L. Doussal, "Classical diffusion of a particle in a one-dimensional random force field," *Annals of Physics*, vol. 201, no. 2, pp. 285 – 341, 1990.

[9] D. K. Lubensky and D. R. Nelson, "Pulling pinned polymers and unzipping dna," *Phys. Rev. Lett.*, vol. 85, pp. 1572–1575, Aug 2000.

[10] D. K. Lubensky and D. R. Nelson, "Single molecule statistics and the polynucleotide unzipping transition," *Phys. Rev. E*, vol. 65, p. 031917, Mar 2002.

[11] D. R. Nelson and N. M. Shnerb, "Non-hermitian localization and population biology," *Phys. Rev. E*, vol. 58, pp. 1383–1403, Aug 1998.

[12] K. A. Dahmen, D. R. Nelson, and N. M. Shnerb, "Population dynamics and non-hermitian localization," in *Statistical mechanics of biocomplexity*, pp. 124–151, Springer, 1999.

[13] Y. Kafri, D. K. Lubensky, and D. R. Nelson, "Dynamics of molecular motors and polymer translocation with sequence heterogeneity," *Biophysical Journal*, vol. 86, no. 6, pp. 3373 – 3391, 2004.

[14] Y. Kafri, D. K. Lubensky, and D. R. Nelson, "Dynamics of molecular motors with finite processivity on heterogeneous tracks," *Phys. Rev. E*, vol. 71, p. 041906, Apr 2005.

[15] N. Hatano and D. R. Nelson, "Localization transitions in non-hermitian quantum mechanics," *Phys. Rev. Lett.*, vol. 77, pp. 570–573, Jul 1996.

[16] N. Hatano and D. R. Nelson, "Vortex pinning and non-hermitian quantum mechanics," *Phys. Rev. B*, vol. 56, pp. 8651–8673, Oct 1997.

[17] N. M. Shnerb and D. R. Nelson, "Winding numbers, complex currents, and non-hermitian localization," *Phys. Rev. Lett.*, vol. 80, pp. 5172–5175, Jun 1998.

[18] P. W. Brouwer, P. G. Silvestrov, and C. W. J. Beenakker, "Theory of directed localization in one dimension," *Phys. Rev. B*, vol. 56, pp. R4333–R4335, Aug 1997.

[19] I. Y. Goldsheid and B. A. Khoruzhenko, "Distribution of eigenvalues in non-hermitian anderson models," *Phys. Rev. Lett.*, vol. 80, pp. 2897–2900, Mar 1998.

[20] J. Feinberg and A. Zee, "Non-hermitian localization and delocalization," *Phys. Rev. E*, vol. 59, pp. 6433–6443, Jun 1999.

[21] S. Alexander, J. Bernasconi, W. R. Schneider, and R. Orbach, "Excitation dynamics in random one-dimensional systems," *Rev. Mod. Phys.*, vol. 53, pp. 175–198, Apr 1981.

[22] D. Hurowitz and D. Cohen, "Nonequilibrium version of the einstein relation," *Phys. Rev. E*, vol. 90, p. 032129, Sep 2014.

[23] L. G. Molinari, "Determinants of block tridiagonal matrices," *Linear Algebra and its Applications*, vol. 429, no. 89, pp. 2221 – 2226, 2008.

ACKNOWLEDGEMENTS

Appendix A: Finding the sign of $V'(0)$

To derive equation (26) we assume an integrated density of states corresponding to equation (3), $\mathcal{N}(\epsilon) = (\epsilon/\epsilon_c)^{\mu}$, where ϵ_c is some cutoff due to the discreteness of the lattice. The electrostatic potential along the real axis is given by (integration by parts of equation (23))

$$V(\epsilon) = -\int_0^{\epsilon_c} \frac{\mathcal{N}(x)}{x - \epsilon} dx \tag{A1}$$

and the derivative with respect to ϵ at the origin is (after integrating by parts)

$$V'(\epsilon) = \int_0^{\epsilon_c} \frac{\rho(x)}{x - \epsilon} dx = \tag{A2}$$

$$= \frac{\mu}{\epsilon_c^{\mu}} \int_0^{\epsilon_c} \frac{x^{\mu-1}}{x - \epsilon} dx = \tag{A3}$$

$$= \frac{\mu}{\epsilon_c^{\mu}} \epsilon^{\mu-1} \int_0^{z_c} \frac{z^{\mu-1}}{z - 1} dz = \frac{\mu}{\epsilon_c^{\mu}} \epsilon^{\mu-1} I(\epsilon) = \rho(\epsilon) I(\epsilon) \tag{A4}$$

where we substituted $z = x/\epsilon$ and defined

$$I(\epsilon) = \int_0^{z_c} \frac{z^{\mu-1}}{z - 1} dz, \quad z_c = \frac{\epsilon_c}{\epsilon} \tag{A5}$$

The integral converges for $\mu < 1$. The integral can be written in terms of Incomplete Euler Beta functions defined as

$$B_u(a,b) = \int_0^u x^{a-1}(1 - x)^{b-1} dx \tag{A6}$$

However one must be careful and take only the Cauchy principal part

$$\lim_{\epsilon \to 0} I = \lim_{\epsilon \to 0} \int_0^{z_c} \frac{z^{\mu-1}}{z - 1} dz = \tag{A7}$$

$$= \lim_{\epsilon \to 0} \lim_{\delta \to 0} \left[\int_0^{1-\delta} x^{\mu-1}(1 - z)^{-1} dz + \int_{1+\delta}^{z_c} z^{\mu-1}(1 - z)^{-1} dz \right] = \tag{A8}$$

$$= \lim_{\epsilon \to 0} \lim_{\delta \to 0} \left[B_{1-\delta}(\mu,0) + \int_{1+\delta}^{z_c} z^{\mu-1}(1 - z)^{-1} dz \right] \tag{A9}$$

$$= \lim_{\epsilon \to 0} \lim_{\delta \to 0} \left[B_{1-\delta}(\mu,0) - \int_{1/z_c}^{1-\delta} t^{-\mu}(1 - t)^{-1} dx \right] \tag{A10}$$

$$= \lim_{\delta \to 0} \left[B_{1-\delta}(\mu,0) - B_{1-\delta}(1 - \mu,0) \right] = \tag{A11}$$

$$= \psi(1 - \mu) - \psi(\mu) = \pi \cot(\pi \mu) \tag{A12}$$

where $\psi(z)$ is the digamma function and the last equality was obtained by the reflection formula. To go from the fourth to the fifth line we took the limit $z_c = \to \infty$, which corresponds to $\epsilon \to 0$. It is clear that C and thus $V'(0^+)$ changes sign from positive to negative at $\mu = 1/2$.

Appendix B: Sliding transition - the definition of s_{μ}

In order to understand the dependence of v and D on N and s, it is useful to recall known results that have been obtained for the time-dependent spreading in an $N = \infty$ lattice. Recall that the drift is induced by the stochastic field, equation (6) whose affinity is defined

$$s = \frac{1}{N} \sum_{n=1}^{N} \mathcal{E}_{n \rightsquigarrow n+1} \tag{B1}$$

The cummulant generating function of the stochastic field can be written as $g(\mu) = (s - s_{\mu})\mu$, where s_{μ} is defined via the following expression:

$$\left\langle e^{-\mathcal{E}\mu} \right\rangle \equiv e^{-(s-s_{\mu})\mu} \tag{B2}$$

If the stochastic field has normal distribution with standard deviation σ, then $s_\mu = (1/2)\sigma^2\mu$. For our box distribution with $\mathscr{E} \in [s - \sigma, s + \sigma]$,

$$s_\mu = \frac{1}{\mu} \ln\left(\frac{\sinh(\mu\sigma)}{\mu\sigma}\right) \tag{B3}$$

which is monotonically ascending from zero to $s_\infty = \sigma$. The positive monotonic function s_μ can be inverted, hence we can define a scaled affinity $\mu(s)$. Note that equation (B2) implies that $\mu(s)$ is the value of μ for which the left-hand-side equals unity.

It has been shown in [7] that the velocity (first moment) exhibits a transition at s_1 from zero to finite veloct. The diffusion (second moment) at s_2 goes from finite to divergent. In the text we showed that the delocalization transition occurs at $s_{1/2}$, which also corresponds to the diffusion coefficient going from sub-ohmic to super-ohmic [22].

Appendix C: The similarity transformation (definition of H)

The associated hermitian matrix H is obtained by a similarity transformation to a basis in which the stochastic field is uniform $\epsilon = s$, followed by setting $s = 0$ on the off diagonals.

$$W = \begin{pmatrix} -\gamma_1 & w_1 e^{\mathscr{E}_1/2} & & w_N e^{-\mathscr{E}_N/2} \\ w_1 e^{-\mathscr{E}_1/2} & \ddots & \ddots & \\ & \ddots & \ddots & w_{N-1} e^{\mathscr{E}_{N-1}/2} \\ w_n e^{\mathscr{E}_N/2} & & w_{N-1} e^{-\mathscr{E}_{N-1}/2} & -\gamma_N \end{pmatrix} \tag{C1}$$

where the decay rates are determined by conservativity

$$\gamma_n = w_{n-1} e^{-\mathscr{E}_{n-1}/2} + w_n e^{\mathscr{E}_n/2} \tag{C2}$$

The following similarity transformation

$$U_{ij} = \delta_{ij} \exp\left[-\frac{1}{2}\sum_{k=1}^{j-1} \mathscr{E}_k + \frac{j-1}{2} s\right], \tag{C3}$$

$$\bar{s} = \frac{1}{N}\sum_{k=1}^{N} \mathscr{E}_k \tag{C4}$$

reduces the rate equation to

$$\tilde{W} = U^{-1}WU = \begin{pmatrix} -\gamma_1 & w_1 e^{\bar{s}/2} & & w_N e^{-\bar{s}/2} \\ w_1 e^{-\bar{s}/2} & \ddots & \ddots & \\ & \ddots & \ddots & w_{N-1} e^{\bar{s}/2} \\ w_n e^{\bar{s}/2} & & -w_{N-1} e^{-\bar{s}/2} & -\gamma_N \end{pmatrix} \tag{C5}$$

The associated hermitian matrix is defined by setting $\bar{s} = 0$,

$$H = \begin{pmatrix} -\gamma_1 & w_1 & & w_N \\ w_1 & \ddots & \ddots & \\ & \ddots & \ddots & w_{N-1} \\ w_n & & -w_{N-1} & -\gamma_N \end{pmatrix} \tag{C6}$$

which is of course real, symmetric and has real eigenvalues ϵ_k.

Appendix D: The formula for the spectral determinant

For the purpose of this section it makes things easier to define $\mathbf{\Gamma} = -W$, the goal is to derive an expression for the spectral determinant

$$\det(\mathbf{\Gamma} - \lambda \mathbf{I}) = 0 \tag{D1}$$

in terms of the hermitian eigenvalues ϵ_k. This determinant can be calculated using a formula due to Molinari [23] for tridiagonal matrices. We define the matrix

$$T_n = \begin{pmatrix} \gamma_n - \lambda & -w_{n-1}^2 \\ 1 & 0 \end{pmatrix} \tag{D2}$$

The key point is that the matrices T_n are the same for $\boldsymbol{\Gamma}$ and for $\boldsymbol{H}$. Using the formula for the determinant for both matrices, we obtain

$$\det(\boldsymbol{H} - \lambda \boldsymbol{I}) = \mathrm{tr}\left[\prod_{n=1}^{N} T_n\right] - 2\left[\prod_{n=1}^{N} w_n\right] \tag{D3}$$

$$\det(\boldsymbol{\Gamma} - \lambda \boldsymbol{I}) = \mathrm{tr}\left[\prod_{n=1}^{N} T_n\right] - 2\left[\prod_{n=1}^{N} w_n\right] \cosh\left(\frac{N\bar{s}}{2}\right) \tag{D4}$$

$$\tag{D5}$$

subtracting the equations and writing the characteristic polynomial of the Hermitian matrix

$$\det(\boldsymbol{H} - \lambda \boldsymbol{I}) = \prod_{n=1}^{N} (\epsilon_n - \lambda) \tag{D6}$$

we obtain an equation for the eigenvalues λ (equation(17))

$$\prod_{n=1}^{N} (\lambda - \epsilon_n) = \left[\prod_{n=1}^{N} w_n\right] 2\left(\cosh\left(\frac{N\bar{s}}{2}\right) - 1\right) \tag{D7}$$

According to Thouless, for the corresponding Hermitian problem

$$e^{N/\xi} = \prod_{n=1}^{N} \left(\frac{\epsilon - \epsilon_n}{w_n}\right) \tag{D8}$$

where $\xi(\epsilon)$ is the energy dependent localization length.

Appendix E: Clean ring

The real spectrum of a clean ring is doubly degenerate. The spectrum is completely complex. The potential oscillates and does not reach the "cosh line" and appears to have $N/2$ maxima. Introducing a small perturbation to one of the bonds, say $g = 1 - \varepsilon$ removes the degeneracy and raises the remaining maxima from $-\infty$.
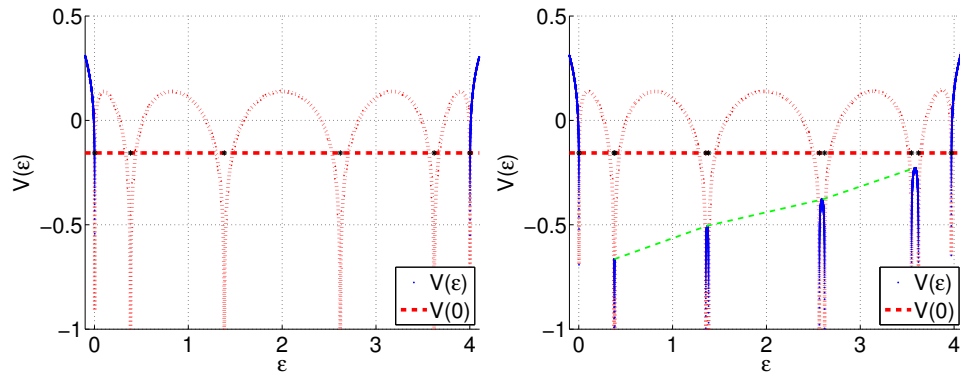

FIG. 8. Solving the secular equation for a clean ring. The left panel shows the electrostatic potential of a clean ring, which is double degenerate. In the right panel one of the bonds is perturbed. Here $N = 10$ and $g = 0.9$ and $s = 0.1$

Appendix F: Ring with weak link "g"

The purpose of this section is to derive equation (39), which is the condition for complexity in a ring with a weak link, in the continuum limit. The ring has circumference L. The dynamics is describes by a diffusion equation with a drift term.

$$\frac{\partial \psi}{\partial t} = \frac{\partial}{\partial x}\left[D(x)\frac{\partial \psi}{\partial x} - u(x)\psi\right] = \frac{\partial}{\partial x}\left[D(x)\frac{\partial \psi}{\partial x}\right] - \frac{\partial}{\partial x}[u(x)\psi] \tag{F1}$$

Assuming that $D(x)$ and $u(x)$ are piecewise constant, the solution to the diffusion equation in each region is simply $\psi \sim e^{-\lambda t + ikx}$, inserting this in equation (F1), we obtain the dispersion relation

$$\lambda = Dk^2 + iuk = D\left(k + \frac{iu}{2D}\right)^2 + \frac{u^2}{4D} \tag{F2}$$

$$k_\pm = \frac{-iu \pm \sqrt{4\lambda D - u^2}}{2D} = \frac{-is}{2} \pm \sqrt{\frac{\lambda}{D} - \frac{s^2}{4}} \tag{F3}$$

$$\equiv \frac{-is}{2} \pm \tilde{k} \tag{F4}$$

So, in each region the solution to equation (F1) is a superposition of clock wise (k_+) and counterclockwise (k_-) waves

$$\psi(x) = Ae^{ik_+x} + Be^{ik_-x} = \tag{F5}$$

$$= e^{\frac{u}{2D}x}\left(Ae^{i\frac{\sqrt{4\lambda D - u^2}}{2D}x} + Be^{-i\frac{\sqrt{4\lambda D - u^2}}{2D}x}\right) \tag{F6}$$

A weak link in the couplings translates to a small region where the diffusion coefficient is much lower than the rest of the ring. We define

$$D(x) = \begin{cases} D_0, & |x| < a/2 \\ D, & |x| > a/2 \end{cases} \tag{F7}$$

To make life simple we define dimensionless variables. The strength of the scatterrer

$$g \equiv \frac{L}{a} \cdot \frac{D_0}{D} \tag{F8}$$

where g is constant in the limit $a \to 0$, $D_0 \to 0$. The quasi momentum $z = \tilde{k}L$ and entropy production $S = sL$. The eigenvalues are

$$\lambda = \frac{D}{L^2}\left(z^2 + \frac{S^2}{4}\right) \tag{F9}$$

Requiring that the diffusion equation equation (F1) be continuous dictates that the distribution function $\psi(x)$ and the current $D(x)\partial_x\psi(x) - v\psi(x)$ be continuous. This is in contrast to the Schroedenger equation, where the continuity requirement is on the derivative $\partial_x\psi(x)$ and not on the current. Let us denote the wave function inside the barrier $|x| < a/2$ as ψ_0. Outside, it is ψ.

$$\psi_0 = Ae^{ik_0x} + Be^{-ik_0x} \tag{F10}$$

$$\partial \psi_0 = ik_0\left(Ae^{ik_0x} - Be^{-ik_0x}\right) \tag{F11}$$

$$\tag{F12}$$

where $k_0 = \sqrt{\lambda/D_0}$. Since we will later take the limit $a \to 0$, we assume that the drift term doesn't play a role within the diffusion barrier.

Inside the barrier, the probability distribution is freely propagating. The values of ψ_0 and $\partial \psi_0$ at each of the boundaries $x = \pm a/2$ can be shown to be related by the linear equation

$$\left.\begin{pmatrix} \psi_0 \\ \partial \psi_0 \end{pmatrix}\right|_{-a/2} = \begin{pmatrix} \cos(k_0 a) & \frac{1}{k_0}\sin k_0 a \\ -k_0\sin k_0 a & \cos(k_0 a) \end{pmatrix}\left.\begin{pmatrix} \psi_0 \\ \partial \psi_0 \end{pmatrix}\right|_{a/2} \tag{F13}$$

And requiring continuity of the distribution and the current, we can stitch the interior solution ψ_0 to the exterior solution ψ

$$\left.\begin{pmatrix} \psi \\ \partial \psi \end{pmatrix}\right|_{-a/2} = \begin{pmatrix} \cos(k_0 a) & \frac{D}{D_0 k_0}\sin k_0 a \\ -\frac{D_0 k_0}{D}\sin k_0 a & \cos(k_0 a) \end{pmatrix}\left.\begin{pmatrix} \psi \\ \partial \psi \end{pmatrix}\right|_{a/2} \tag{F14}$$

Taking, carefully, the limit $a \to 0$,

$$\left.\begin{pmatrix} \psi \\ \partial \psi \end{pmatrix}\right|_{-a/2} \approx \begin{pmatrix} 1 & D\frac{a}{D_0} \\ 0 & 1 \end{pmatrix} \left.\begin{pmatrix} \psi \\ \partial \psi \end{pmatrix}\right|_{a/2} \tag{F15}$$

rewriting these two equations explicitly, we obtain the diffusion barrier matching conditions

$$\psi(a/2) - \psi(-a/2) = -\frac{a}{D_0} D \partial \psi(a/2) \tag{F16}$$

$$\partial \psi(a/2) = \partial \psi(-a/2) \tag{F17}$$

To check, notice that if $D_0 \to 0$ faster than $a \to 0$, Neumann boundary conditions are recovered.
If $D_0 = D$, periodic boundary conditions are recovered. The matching conditions of equation (F16) can be written in matrix form with the matching matrix M

$$M = \begin{pmatrix} 1 & D\frac{a}{D_0} \\ 0 & 1 \end{pmatrix} \tag{F18}$$

The transfer matrix across a segment of length L with bias s is

$$T(s,k;L) \equiv \frac{e^{sL/2}}{k} \begin{pmatrix} -\frac{s}{2}\sin(kL) + k\cos(kL) & \sin(kL) \\ -\left(\frac{s^2}{4}+k^2\right)\sin(kL) & \frac{s}{2}\sin(kL) + k\cos(kL) \end{pmatrix} \tag{F19}$$

Using the matching conditions of equation (F16) and the solution of the form of equation (F5), together with periodic boundary conditions, we have

$$\left.\begin{pmatrix} \psi \\ \partial \psi \end{pmatrix}\right|_{x=0} = TMT \left.\begin{pmatrix} \psi \\ \partial \psi \end{pmatrix}\right|_{x=0} \tag{F20}$$

A non trivial solution is possible only if

$$\det(TMT - I) = 0 \tag{F21}$$

which leads to the secular equation

$$\cos(\tilde{k}L) + \alpha \frac{\lambda}{2\tilde{k}} \sin(\tilde{k}L) = \cosh(sL/2) \tag{F22}$$

where $\alpha = \frac{a}{D_0}$, which can also be written simply as

$$\sqrt{1 + \alpha^2 \frac{\lambda^2}{4\tilde{k}^2}} \cos\left[\tilde{k}L - \arctan\left(\alpha\frac{\lambda}{2\tilde{k}}\right)\right] = \cosh(sL/2) \tag{F23}$$

where

$$\tilde{k} \equiv k + \frac{is}{2} = \sqrt{\frac{\lambda}{D} - \frac{s^2}{4}} \tag{F24}$$

In more conventional notations, equation (F22) can be written as follows

$$\cos(\gamma(\lambda)) = \sqrt{g(\lambda)} \cosh\left(\frac{sL}{2}\right) \tag{F25}$$

where

$$g(\lambda) = \left[1 + \left(\frac{\lambda}{2\tilde{k}}\alpha\right)^2\right]^{-1}, \quad \gamma(\lambda) = \tilde{k}L - \arctan\left(\frac{\lambda}{2\tilde{k}}\alpha\right) \tag{F26}$$

Alternatively, the secular equation can be written in the form

$$\cos\left(L\sqrt{\frac{\lambda}{D} - s^2/4}\right) + \frac{1}{2}\frac{a}{D_0}\frac{\lambda}{\sqrt{\frac{\lambda}{D} - s^2/4}}\sin\left(L\sqrt{\frac{\lambda}{D} - s^2/4}\right) = \cosh\left(\frac{sL}{2}\right) \tag{F27}$$

or in terms of dimensionless variables

$$\cos(z) + \frac{1}{g}\frac{z^2 + (\frac{S}{2})^2}{2z}\sin(z) = \cosh\left(\frac{S}{2}\right) \tag{F28}$$

1. Ground state of associated hermitian problem

The eigenvalues of the associated hermitian problem are (in analogy with the definition of H)

$$\epsilon_k = D\left(k^2 + \frac{s^2}{4}\right) \tag{F29}$$

and k is determined by the secular equation equation (F27) with $s = 0$ on the right hand side. This leads to the equation

$$\cos(z_\epsilon) + \frac{1}{g}\frac{z_\epsilon^2 + (\frac{S}{2})^2}{2z_\epsilon}\sin(z_\epsilon) = 1 \tag{F30}$$

where we have defined $z_\epsilon = kL$. If $S = 0$, then $\epsilon_k = \lambda_k$, so when S is small we expect some correction Thus, we expand equation (F30) around $z_\epsilon = iS/2$ which corresponds to $\lambda = 0$, expand in powers of S and solve for z_{ϵ_0} to obtain

$$z_{\epsilon_0}^2 = \frac{S^2}{4}\frac{1}{g-1} \tag{F31}$$

and from equation (F39)

$$\epsilon_1 = \frac{S^2}{4}\frac{g}{g-1} \tag{F32}$$

2. The spectrum

To characterize the spectrum vs. s, it is good to keep in mind two limiting cases. When $g = 1$, we have a clean ring, and all eigenvalues are complex and they form a gapless continuum. When $g = 0$, we have a chain, where all the eigenvalues are real. In this case there is a gapped continuum that begins at $\Gamma = s^2/4$.

For finite g, the spectrum is gapped, however a "bubble" of complex eigenvalues can appear in the continuum. We obtain an analytical expression for the gap when the spectrum is real and prove that the gap is finite even when there are complex eigenvalues in the spectrum.

Let us assume that λ is real. For given S, the left hand side of the secular equation equation (F27) is oscilliatory, provided $\lambda > S^2/4$, otherwise, the trigonometric functions become hyperbolic. The oscillations are within an envelope function $\kappa(\lambda)$,

$$\kappa(\lambda) = \sqrt{1 + \frac{1}{g^2}\frac{\lambda^2}{4\lambda - S^2}} \tag{F33}$$

There are real solutions to the secular equation as long as the envelope function satisfies

$$\kappa(\lambda) > \cosh\left(\frac{S}{2}\right) \tag{F34}$$

which leads to the expression for the gap, provided that the spectrum is entirely real (Fig.9),

$$\mathrm{Re}[\lambda] \geq 2g^2\sinh^2(S/2)\left[1 + \sqrt{1 - \frac{S^2}{4g^2\sinh^2(S/2)}}\right] = \Delta(s) \tag{F35}$$

When S increases such that $\cosh(S/2) > \kappa(\lambda)$, a complex "bubble" of eigenvalues appears. The bubble structure is due to the fact that the envelope function $\kappa(\lambda)$ has a global minimum at $\lambda_{\min} = S^2/2$, so for $\lambda > \lambda_{\min}$ the envelope function grows monotonically and will eventually intersect with $\cosh(S/2)$. This scenario is illustrated in Fig.10. The minimum value of the envelope function is

$$\kappa_{\min} = \sqrt{1 + \left(\frac{S}{2g}\right)^2} \tag{F36}$$

The critical value S_g such that for $S > S_g$ there are complex eigenvalues in the spectrum is determined by the transcendental equation (equation (39))

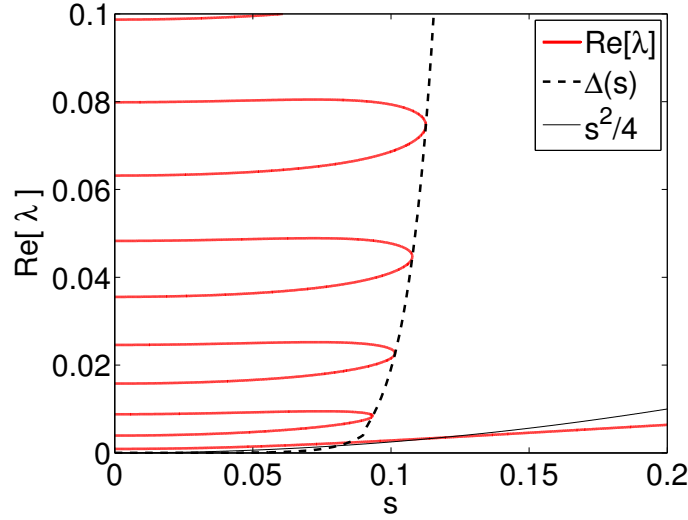$$1 + \left(\frac{S}{2g}\right)^2 = \cosh^2\left(\frac{S}{2}\right) \tag{F37}$$

FIG. 9. The real part of the eigenvalues for an $L = 100$, $D = 1$ ring with a single diffusion barrier with $g = 10^3$ plotted vs. the affinity s. The dashed black line is equation (F35), which is the value of the gap and also indicates where the eigenvalues become complex. Notice that at the bottom of the band there is an eigenvalue that is always real. This plot was generated by producing a contour plot of equation (F27) for real λ's, it shows only real eigenvalues.

3. Proof the gap is finite

To show that the gap remains finite even when there are complex eigenvalues, it is more convenient to use the second form of the secular equation where the wave vector is $z = x + iy$. The eigenvalues can be expressed in the following form

$$\lambda = (x+iy)^2 + \left(\frac{S}{2}\right)^2 = x^2 - y^2 + \left(\frac{S}{2}\right)^2 + 2ixy \tag{F38}$$

There is a trivial eigenvalue at $x = 0$, $y = S/2$. To show that the gap is finite, it is sufficient to show that for $x \neq 0$, $y < S/2$. Inserting $z = x + iy$, the secular equation splits in to two equations (for real and imaginary parts). The real part of equation equation (26) is

$$\cos(x)\left[\cosh(y) - \frac{y}{g}\sinh(y)\frac{x^2+y^2-S^2/4}{2(x^2+y^2)}\right] + \tag{F39}$$

$$+ \sin(x)\left[gx\cosh(y)\frac{x^2+y^2+S^2/4}{2(x^2+y^2)}\right] = \cosh\left(\frac{S}{2}\right) \tag{F40}$$

This equation has the form $A(x,y)\sin(x) + B(x,y)\cos(x) = \cosh(S/2)$. For finite $x = x_1$, y_1 is determined by the condition that the envelope of the function intersects with $\cosh(S/2)$

$$\sqrt{A^2 + B^2} = \cosh(S/2) \tag{F41}$$

To prove that $y_1 < S/2$ it is enough to show that for $y = S/2$ the envelope satisfies $\sqrt{A^2 + B^2} > \cosh(S/2)$. Assume that $g \gg 1$ and $S \gg S_g$, in this case there is a large bubble of complex eigenvalues so the gap is complex. Also, we can approximate $\cosh y \approx \sinh y \approx e^y$ and $\cosh(S/2) \approx e^{S/2}$. In this limit the envelope is

$$\left.\frac{1}{2g}e^y\sqrt{x^2+y^2}\sqrt{1 + \frac{S^2(x^2-y^2+S^2)}{2(x^2+y^2)}}\right|_{y=S/2} = \tag{F42}$$

$$\frac{e^{S/2}}{2g}\sqrt{x^2+(S/2)^2}\sqrt{1 + \frac{S^2(x^2+3(S/2)^2)}{2(x^2+(S/2)^2)}} > e^{S/2} \tag{F43}$$
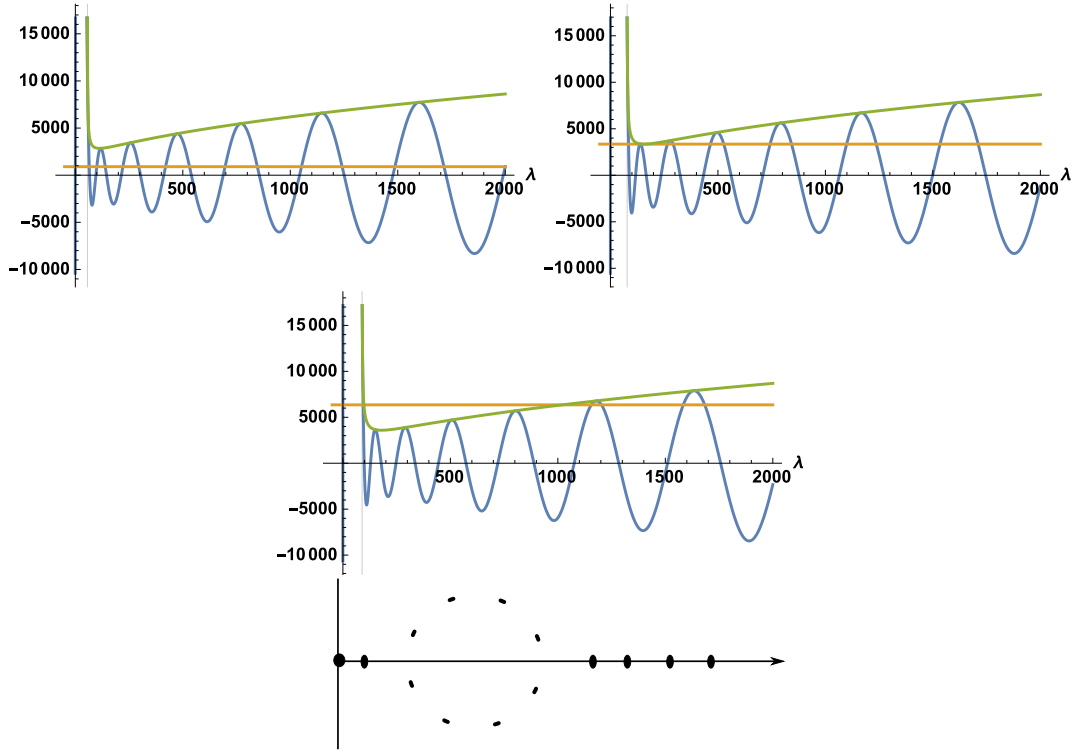
so the solution must be $y < S/2$.

FIG. 10. The secular equation $f(\lambda) = \cosh(S/2)$ for $g = 1/380$, so $S_g = 17.6$. Top row: (left) $S = 15$, all eigenvalues are real. (right) $S = S_g$, marginal case. Middle row:l $S = 19$, the fully developed scenario, where the spectrum is initially real, then there is a "bubble" of complex eigenvalues and then the spectrum becomes real again. The high eigenvalues correspond to modes that decay very fast. Intuitively, since the high eigenvalues decay quickly, they cannot complete a trip around the ring before they decay, so they must be real. The blue line is the oscillating part of the secular equation. The green line is the envelop function and the horizontal orange line is $\cosh(S/2)$. In the bottom row we draw a schematic diagram of the spectrum in the complex plane of λ, corresponding to the fully developed scenario.

Appendix G: Ring with single field defect

The field defect of the discrete ring translates to a defect in the velocity field in the continuum limit. We define a region $|x| < a/2$ in which the velocity field is different. For $|x| > a$ we have $u/D = s$ and for $|x| < a$ we have $u/D = s + \sigma$. Note that for there to be a transition from real to complex s and σ must have opposite signs. The boundary conditions are that the wave function and the current be continuous everywhere. Applying the boundary conditions across the defect and taking the limit $a \to 0$ such that $a\sigma = \Sigma(\text{const})$ we obtain the matching matrix at each boundary of the defect

$$M_{\pm} = \begin{pmatrix} 1 & 0 \\ \pm\sigma & 1 \end{pmatrix} \tag{G1}$$

where M_+ is at $x = a/2$ and M_- at $x = -a/2$. The transfer matrix is along a distance x is $UT(x)U^{-1}$ where

$$U = \begin{pmatrix} 1 & 1 \\ ik + \frac{is}{2} & -ik + \frac{is}{2} \end{pmatrix} \tag{G2}$$

and

$$T = \begin{pmatrix} e^{i\left(k - \frac{is}{2}\right)x} & 0 \\ 0 & e^{i\left(-k - \frac{is}{2}\right)x} \end{pmatrix} \tag{G3}$$

Note that inside the defect $s \to s + \sigma$ and $k \to \sqrt{\lambda/D - (s + \sigma)^2/4}$ while outside the defect $s \to s$ and $k \to \sqrt{\lambda/D - s^2/4}$. The matching condition between two sides of the defect is obtained by propagating the wave between the edges of the defect and taking the limit $a \to 0$ while keeping $a\sigma$ constant,

$$\mathcal{M} = \lim_{a \to 0} M_- UT(a)U^{-1}M_+ = \begin{pmatrix} e^{\Sigma} & 0 \\ (-1 + e^{\Sigma})s & 1 \end{pmatrix} \tag{G4}$$

For a ring the wave function must obey

$$\left.\begin{pmatrix} \psi \\ \partial \psi \end{pmatrix}\right|_{x=0} = T(L/2)\mathscr{M}T(L/2)\left.\begin{pmatrix} \psi \\ \partial \psi \end{pmatrix}\right|_{x=0} \tag{G5}$$

which is possible only if

$$|T(L/2)\mathscr{M}T(L/2) - I| = 0 \tag{G6}$$

This is the secular equation, which takes the explicit form

$$\cos\left(\frac{1}{2}\sqrt{4\lambda - S^2}\right)\cosh\left(\frac{\Sigma}{2}\right) + \frac{\sin\left(\frac{1}{2}\sqrt{4\lambda - S^2}\right)}{\sqrt{4\lambda - S^2}}S\sinh\left(\frac{\Sigma}{2}\right) = \cosh\left(\frac{S+\Sigma}{2}\right) \tag{G7}$$

It is easy to verify that $\lambda = 0$ is a solution as required. The envelope function is

$$\kappa(\lambda) = \sqrt{\cosh^2\left(\frac{\Sigma}{2}\right) + \frac{S^2}{4\lambda - S^2}\sinh^2\left(\frac{\Sigma}{2}\right)} \tag{G8}$$

with $\kappa(0) = \cosh((S+\Sigma)/2)$. The envelope function is monotonically decreasing for $\lambda > S^2/4$ reaching an asymptotic value

$$\lim_{\lambda\to\infty}\kappa(\lambda) = \cosh\left(\frac{\Sigma}{2}\right) \tag{G9}$$

Note that the true envelope function does not really explode at $\lambda = S^2/4$, because $\sinh(x)/x \to 1$ as $x \to 0$. The condition for complexity is that

$$\kappa(0) > \kappa(\infty) \tag{G10}$$

So S_c is defined by the equation

$$\cosh\left(\frac{S+\Sigma}{2}\right) = \cosh\left(\frac{\Sigma}{2}\right) \tag{G11}$$

As defined in the text, the affinity is the mean of the stochastic field, $s = (S+\Sigma)/L$, thus the equation has a solution at $sL = \Sigma$

$$s_c L = \sigma a \implies s_c = \frac{\sigma}{N} \tag{G12}$$

as in equation (31) of the text.

Appendix H: Ring with sparse disorder

Appendix I: Ring with white disorder (French)

Appendix J: Step by step electrostatics

The building blocks of the analysis are an isolated state, or point charge and a continuum. From these blocks we can construct any relevant 2D electrostatic potential.

Point charge-. The potential of a single charge is simply

$$V_{\text{charge}}(R) = \ln|R - \epsilon_1| \tag{J1}$$

Uniform charge-.

Continuum (clean ring)-. The associated hermitian spectrum of a clean lattice ring is obtained by appropriately setting $s = 0$ in equation (12)

$$\epsilon_n = 2w\left[\cosh\left(\frac{s}{2}\right) - \cos\left(\frac{2\pi}{N}n\right)\right] \tag{J2}$$

which can be inverted to obtain the integrated density of states

$$\mathscr{N}(\epsilon) = \frac{N}{2\pi}\arccos\left[\cosh\left(\frac{s}{2}\right) - \frac{\epsilon}{2w}\right] \tag{J3}$$

The density of states is

$$\rho(\epsilon) = \frac{d\mathcal{N}}{d\epsilon} = \frac{N}{4\pi w} \left[1 - \left(\cosh\left(\frac{s}{2}\right) - \frac{\epsilon}{2w} \right)^2 \right]^{-1/2} \tag{J4}$$

from which we obtain

$$\rho(k) = \frac{N}{4\pi w} \left[1 - \cos^2(k) \right]^{-1/2} = \frac{N}{4\pi w \sin(k)} \tag{J5}$$

The electrostatic potential formed by a charge distribution $\rho(\epsilon)$ is given by means of equation (23)

$$V(R) = \int_a^b \ln \left| \frac{\epsilon - R}{w} \right| \rho(\epsilon) d\epsilon = \frac{N}{2\pi} \int_0^{2\pi} \ln \left| 2\cosh\left(\frac{s}{2}\right) - 2\cos(k) - R \right| dk = \tag{J6}$$

where $[a,b] = 2w[\cosh(s/2) \pm 1]$. The potential is an oscillating function but the peaks form an envelope function that has the values

$$V_{\text{continuum}}(R) \approx \frac{N\ln(2)}{\pi} + \begin{cases} \frac{N}{2\pi} \sqrt{|R-a|} & , \ R < a \\ \\ 0 & , \ R > a \end{cases} \tag{J7}$$
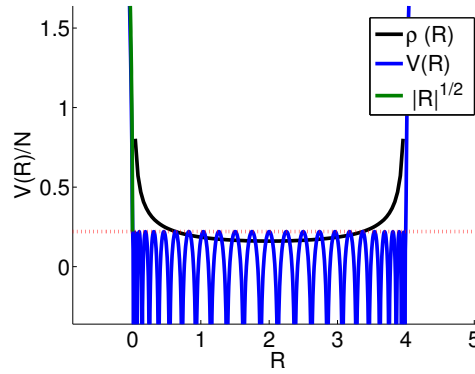

FIG. 11. The electrostatic potential of a clean ring, equation (J7) (blue). The potential is flat (dashed red line) where the density of states (black curve) is not zero and diverges as $\sqrt{|R|}$ elsewhere (green line)